ELSEVIER

Journal of Volcanology and Geothermal Research 66 (1995) 101–113

Journal of volcanology and geothermal research

Textural difference between pahoehoe and aa lavas of Izu-Oshima volcano, Japan — an experimental study on population density of plagioclase

Hiroaki Sato

Department of Natural Environmental Sciences, Faculty of Integrated Arts and Sciences, Hiroshima University, Higashi-Hiroshima, 724 Japan

Received 27 June 1991; accepted in revised form 7 July 1994

Abstract

The groundmass textures of 1778 A.D. pahoehoe and 1986 A.D. aa lavas of Izu-Oshima volcano, Japan, differ in population density of plagioclase by about two orders of magnitude. The pahoehoe lavas are coarser grained and have a population density of $10^{7.0}$ cm^{-3}, while the aa lavas are finer grained and have a population density of $10^{9.3}$ cm^{-3}. The groundmasses of these texturally different lavas, however, have nearly the identical chemical compositions. One-atmosphere melting/crystallization experiments on the lavas showed that a 20°C difference in initial-melting temperature near the liquidus temperature can cause about five orders of magnitude difference in the population density of plagioclase after annealing at about 100°C below the liquidus temperature. Yet, more than two orders of magnitude difference in cooling rate of the experiments only bring about less than one order of magnitude difference in population density. The large effect of the initial-melting temperature on the population density of plagioclase is interpreted to reflect nucleation induced by the transformation of polymerized clusters in the melt into crystal nuclei by a reduction in the critical size of the nuclei; the initial size distribution of clusters in the melt largely affects the population density of plagioclase. During natural eruptive processes, degassing of magmas produces strongly undercooled conditions, and it is proposed that a slight difference in the degree of undercooling of magmas before final degassing and eruption may have caused the large difference in the population density of plagioclase of the pahoehoe and aa lavas.

1. Introduction

Dualistic morphology of basaltic lavas is well known, i.e., pahoehoe and aa (e.g., Macdonald, 1972). Much of the discussion on the origin of the differences of these lavas has centered on the relative role of cooling rate, viscosity and rate of shear strain of lavas (Peterson and Tilling, 1980; Kilburn, 1981; Rowland and Walker, 1990). It is commonly suggested that degassing is related somehow to the apparent viscosity of lava, which, in turn, may be related to groundmass texture because degassing raises equilibrium liquidus temperature and promotes crystallization (Sparks and Pinkerton, 1978; Lipman et al., 1985). However, little work has been carried out on the petrographic characteristics of the lavas in relation to the morphology, even though Kilburn (1987) already has demonstrated high-plagioclase content in the groundmass of aa lavas and suggested that the entanglement of plagioclase laths in the groundmass of aa lavas may contribute to the high apparent viscosity.

In a textural investigation of the eruption products of Izu-Oshima volcano, central Japan, I found that the population density of plagioclase differs by more than

SSDI 0377-0273(94)00055-7

two orders of magnitude between pahoehoe and aa lavas. Groundmass plagioclase in pahoehoe lavas has smaller population density and is much more coarser grained than plagioclase in aa lavas. Yet, the two lava types have virtually the same groundmass chemical compositions. I further conducted melting/crystallization experiments to evaluate quantitatively the effects of cooling rate and initial-melting temperatures on plagioclase population density. These are the major parameters that affect the textural development of basaltic magmas, as demonstrated by the 1-atmosphere melting/crystallization experiments of Lofgren (1980, 1983). My experiments show that variation in cooling rate cannot cause the wide range of the plagioclase population density observed in natural pahoehoe and aa lavas, whereas a slight change in initial-melting temperature around the liquidus temperature can cause more than five orders of magnitude difference in the population density and can account for the wide variations of plagioclase population density seen for natural lavas. The experimental results suggest that the pahoehoe lavas were less undercooled before degassing and eruption than were the aa lavas.

2. Population density of plagioclase in pahoehoe and aa lavas of Izu-Oshima volcano

The lavas of the younger period of Izu-Oshima volcano show a wide range in the groundmass textures in terms of size and population density of plagioclase (Fig. 1). The finer-grained 1986LA lava (Fig. 1B) is characterized by aa to block surface features, whereas the coaser-grained 1778 lava (Fig. 1A) exhibits macroscopic pahoehoe surface characteristics. Among the lavas of the younger period, the 1950 A.D. lava flows are mostly pahoehoe and have a coarse-grained groundmass similar to that of the 1778 lava; in contrast, most of the lavas of other large eruptions of the volcano (1–0.1 km^3, Nakamura, 1964) are fine grained and have a high population density of plagioclase resembling those of the 1986LA aa or block lavas.

To quantitatively characterize the textures of these basalts, I measured the population density of plagioclase, i.e., the total number of plagioclase crystals in a cubic centimeter. Because plagioclase is the dominant phase in the groundmass of basalts of Izu-Oshima volcano and represents the liquidus phase at low pressures,

Fig. 1. Photomicrographs of pahoehoe and aa lavas of Izu-Oshima volcano. Bars (lower left corner) are 0.1 mm. (A) Near the surface of the 1778 pahoehoe lava flow. (B) Upper clinker block of 1986LA aa or block lava flow.

its size and population density essentially determine the textural characteristics of the basalts.

Measurement of population density was done with an optical microscope using thin sections of the lavas, and with optical microscope images or back-scattered electron images of polished thin sections for synthetic samples. First, I measured length(l_2) and width(l_1) of all plagioclase laths contained within an area by means of a digitizer and an image-analyzing system (Nikon COSMOZONE 1SA). Then I obtained a frequency histogram of radii of equi-area circles. In Fig. 2 an example is shown of such a frequency histogram for 1778 A.D. pahoehoe lava. The two-dimensional population density thus obtained was converted to a three-dimensional population density by using the equation of Gray (1970), $Z = (\pi\alpha)^{1/2} \times N/4r$, where Z and N

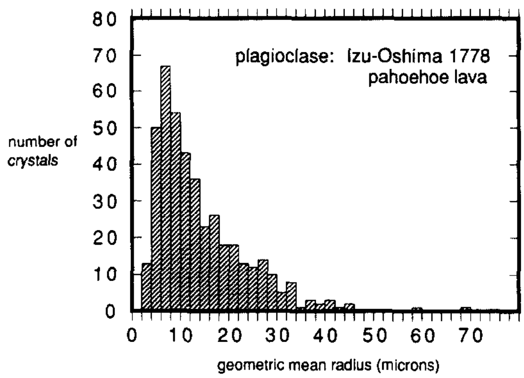

Fig. 2. Crystal-size distribution (CSD) of plagioclase in the groundmass of the 1778 pahoehoe lava flow of Izu-Oshima volcano. Calculating of the number density of plagioclase is discussed in the text.

represent population density of tabular crystals in three and two dimensions, respectively. α denotes the aspect ratio (length/width ratio) and r is the radius of the equi-area circle of the lath. Although Kirkpatrick (1978) preferred a 3/2 power integration to obtain the three-dimensional population density from two-dimensional data, the above equation gives a more precise data conversion (Gray, 1978). The population density of each size class was calculated assuming the average radius corresponding to the middle of the range, and the total population density of plagioclase was obtained by the summation of those for each size range (Table 1). The average size (mean radius of equi-area circle) of plagioclase is 14 and 3 μm for 1778 and 1986LA lavas, and the population density of plagioclase is $10^{7.0}$ and $10^{9.3}$ cm^{-3}, respectively. The bulk-rock chemical analyses of these lavas are shown in Table 2. Slight differences in bulk composition mostly reflects the

Table 1
Measurement of number density of plagioclase (Z) in natural lavas

Lava	No.	Area (mm^2)	l_1 (μm)	l_2 (μm)	α	r (μm)	vol.%	log(Z) (cm^{-3})	Method
Pahoehoe 1778	424	2.78	14.9	43.2	2.99	13.8	10.4	6.97	OPT[a]
Aa 1986LA	474	0.107	2.9	11.2	4.07	3.07	18.0	9.29	OPT

No. = number of crystals measured; l_1 = mean width; l_2 = mean length; α = mean aspect ratio; r = average geometric-mean radius; Z = number density of plagioclase.
[a]Measurement by optical microscope.

Table 2
Bulk-rock chemistry of the samples[a]

Sample	1778 pahoehoe	1986LA(a) aa (A)[b]	1986B bomb (B)[b]
No.[c]	5	4	5
SiO_2	52.95(16)	52.56(9)	54.16(32)[d]
TiO_2	1.42(3)	1.29(3)	1.36(1)
Al_2O_3	13.58(3)	14.54(8)	13.95(12)
FeO	12.93(12)	11.97(15)	12.44(27)
MnO	0.20(2)	0.20(3)	0.20(2)
MgO	4.62(4)	4.61(3)	4.05(5)
CaO	9.63(8)	10.06(6)	8.87(7)
Na_2O	2.16(6)	2.03(4)	2.30(2)
K_2O	0.46(1)	0.40(1)	0.45(1)
total	97.95	97.66	97.78

[a]Analyses were made on fused glass beads by electronprobe microanalyzer. The low totals are partly due to the data-reduction method assuming iron as ferrous. About 90% of the iron is ferric in the actual beads.
[b]Starting materials for the experiments (see Table 3).
[c]Number of analyzed spots.
[d]Numbers in parenthes denote the standard error of the last decimal units cited.

presence of several percents of plagioclase phenocryst in 1986LA lavas; the groundmass compositions of these lavas are nearly the same (Nakano and Yamamoto, 1991). From the size–frequency data, we can obtain CSD (crystal size distribution) data (Fig. 3). The CSD plotting method has been introduced to textural analyses of rocks by Marsh (1988) and Cashman and Marsh (1988), and applied to investigate the crystallization history of some volcanic rocks (Cashman, 1988; Mangan, 1990). Figure 3 shows that the ground-

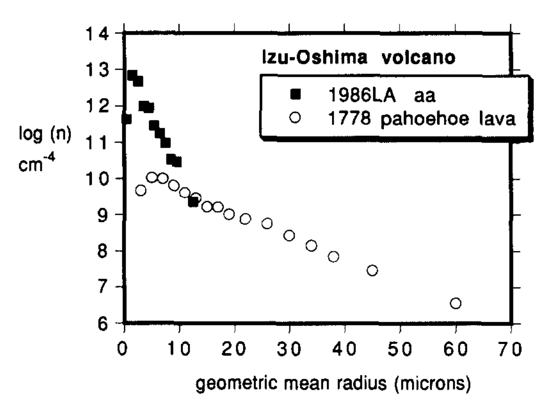

Fig. 3. CSD plot of the 1778 pahoehoe and 1986 LA aa lavas of Izu-Oshima volcano. The data show linear relations with different slopes. See the text for discussion.

mass textures of the pahoehoe and aa lavas have linear CSD curves, with the slope for the aa lava much steeper than that for the pahoehoe lava. The significance of the difference in slopes and intercepts of the CSD curves for the pahoehoe and aa lavas is discussed later.

Degraff et al. (1989) reported an example of textural variation in groundmass within a lava flow section. In general, the groundmass texture become more crystalline toward the center of a lava flow. The natural lavas used for the textural analyses in this study (Table 1), however, are obtained from the surface of lava flows. Thin section examination of other samples from lava flows of the 1778, 1950 and 1986 A.D. eruptions of Izu-Oshima volcano, revealed that the textural difference observed between the surface samples of pahoehoe and aa lava flows holds also for samples from flow interiors; i.e., plagioclase microlites are slightly larger but have nearly the similar population density in the center of the lavas as in the margin of the lavas. Presence of some crystallites in the groundmass in the central part of the lava flows made the precise measurement of population density of plagioclase difficult for such samples. It seems that positions of samples within a lava flow, representing different cooling rates on the surface, do not account for the strong contrast of the groundmass texture between the samples of pahoehoe and aa lavas studied.

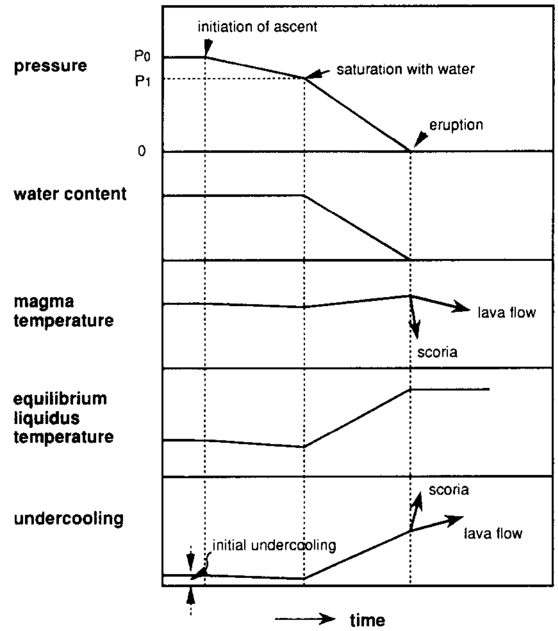

Fig. 4. A schematic model of variations of physical properties of magmas before and during eruption. The time–undercooling relation is simulated in the experiments.

3. A model of magmatic conditions during eruption

Before considering the experimental studies, I briefly discuss a model of crystallization of magmas during eruption, which is relevant to the formation of groundmass textures. There are three possible driving forces for eruption (Aramaki, 1975): (a) buoyancy of magmas against country rocks; (b) pressure increase due to exolution of volatiles in the chamber (Blake, 1984); and (c) tectonic stress acting on the chamber. Among these factors, tectonic stress can trigger volcanic eruptions or somewhat affect eruptive sequences, but they alone may not produce large eruptions because crustal rocks do not show high compressibility and would not sustain high stress before failure by brittle fracture.

Most basalts and andesites have 1–3 wt.% of water (Sekine et al., 1979), which correspond to a saturation depth of less than 3 km (Burnham, 1974). Magma chambers beneath basaltic-andesitic volcanoes are generally considered to be more than 3 km deep, and basalt to andesite magmas may not be saturated with water in such chambers. In this case, the most important driving force for initiation of eruption is buoyancy of magmas, and once a magma rises and reaches a water-saturation depth, the mode of vesiculation and degassing will essentially determines the eruptive style. If magma contains abundant CO_2 along with water, the saturation depth can be much deeper (e.g., Stolper and Holloway, 1988). However, because the pressure dependence of the solubility of CO_2 in magma is small, only small excess pressure due to vesiculation within near-surface chambers can be expected. On the other hand, silicic melts are mostly saturated with water within the upper part of magma chambers (Aramaki, 1971; Rutherford et al., 1985), and eruption may be initiated by the overpressure due to vesiculation as proposed by Blake (1984); an eruption also may be triggered by an increase in buoyancy force associated with low densities of vesiculated magmas (Ida, 1990).

A schematic model of variation in physical properties of magmas before and during eruption of basaltic magmas is depicted in Fig. 4. Initially, the magmas are not saturated with water, and its ascent may be driven by input of magmas from below. At a certain depth, corresponding to P_1 in Fig. 4, the magma becomes oversaturated with water and begins to vesiculate. Under real conditions, the ascent velocity of magmas may increase as magmas rise (Jaupart and Allegre, 1991); however, for simplicity, I assumed constant ascent velocity. The degassing rate is also assumed to be constant during magma rise. Magmatic temperatures decrease slightly by adiabatic decompression under water-undersaturated conditions, and may increase slightly during vesiculation because of the heat of exolution of water and of crystallization (Nicholls and Stout, 1982), related to an increase of liquidus temperature. The equilibrium-liquidus temperature decreases as pressure decreases before water saturation, but increases abruptly during water exolution. The degree of undercooling of magmas slightly decreases during ascent without water exolution, but then rapidly increases during the later stages accompanied by water exolution. In Fig. 4, I assume that cooling by heat conduction is negligibly small in the intratelluric conditions, and that heat conduction is the controlling factor on the temperature as well as degree of undercooling once magma reaches the surface.

Rock textures may record the time sequence of the degree of undercooling of magmas, since crystallization is promoted by undercooling of magmas. Undercooling is induced either by degassing or heat loss by conduction. The former effect can be estimated by the difference between the equilibrium-liquidus temperature under water-free condition and actual temperature of magmas estimated from mineralogical thermometry, i.e., 50–100°C for basaltic rocks of Izu-Oshima volcano (Sato, unpublished data), 100–200°C for andesites (Sekine et al., 1979), and 200–400°C for dacite and rhyolite (Aramaki, 1971; Rutherford et al., 1985). This effect can cause 20–100% crystallization even when we take the heat of crystallization into account, because 1-atmosphere melting intervals of magmas are mostly 150–300°C. Some glassy lavas such as obsidian may be formed by large undercooling of magmas during degassing as suggested by Swanson et al. (1989). The following experimental study was designed to simulate the time span of undercooling of magmas illustrated in Fig. 4.

4. Experimental studies of the population density of plagioclase

Lofgren (1980, 1983) experimentally demonstrated that textures of basaltic rocks are mainly determined by the initial-melting temperature near liquidus temperature as well as cooling rate, and melt compositions. Basalts of Izu-Oshima volcano show a wide range of population density of plagioclase, even though they have rather uniform groundmass major-element chemistry (Table 2). My experiments attempt to evaluate quantitatively the effects of cooling rate and initial-melting temperatures on the population density of plagioclase.

Both linear cooling experiments and isothermal cooling experiments were conducted using the 1986 eruption products of Izu-Oshima volcano (Fig. 5). Table 2 shows the bulk-rock chemistry of 1986LA lava and 1986B bomb samples used as starting materials in the experiments. The time–undercooling relations in the experiments are assumed to approximate the time–undercooling relations of natural eruptions as shown in Fig. 4. In actual magmatic processes undercooling is mainly controlled by degassing of volatiles (mostly water) during eruption, whereas in the experiments undercooling is induced by changing the melt temperature relative to 1-atmosphere equilibrium-liquidus temperatures. The wire-loop method was used to hold and drop the samples (Presnall and Brenner, 1974).

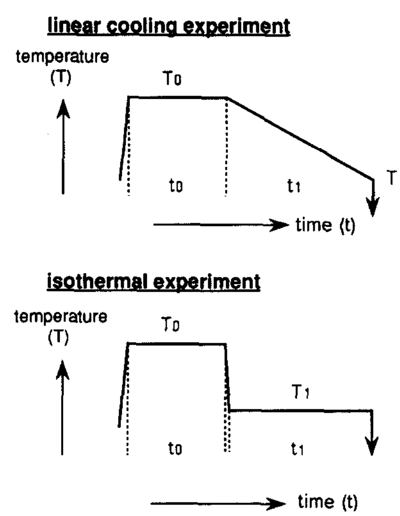

Fig. 5. Temperature–time relations of linear cooling and isothermal crystallization experiments.

Table 3
Experimental run conditions

Starting material	Run number	T_0 (°C)	t_0 (h)	T_1 (°C)	t_1 (h)
Linear cooling experiments					
B	#183A	1200	1.0	1100	10.0
B	#182A	1200	1.0	1100	2.0
B	#176A	1200	1.0	1100	0.5
B	#177A	1190	1.0	1100	0.5
B	#184A	1180	1.0	1100	0.5
A	#183B	1200	1.0	1100	10.0
A	#176B	1200	1.0	1100	0.5
A	#175B	1200	10.0	1100	0.5
A	#178B	1210	1.0	1100	0.5
A	#179B	1200	1.0	1050	0.083
Isothermal experiments					
B	#187A	1200	1.0	1100	1.0
B	#186A	1200	1.0	1100	13.4
B	#188A	1190	1.0	1100	1.0
B	#180A	1190	1.0	1100	13.0
B	#185A	1180	1.0	1100	1.0
B	#189A	1180	1.0	1100	13.6

The meanings of T_0, t_0, T_1 and t_1 of both linear cooling experiments and isothermal experiments are shown in Fig. 5.

The furnace temperature is calibrated against melting points of gold and diopside at the charge site, and is accurate within 3°C. The furnace atmosphere is controlled by mixing CO_2 and H_2 gases with a constant volume ratio of 48, which corresponds to 0–1 log unit higher oxygen fugacity compared with those buffered by a fayalite–magnetite–quartz assemblage. This redox state coincides with the redox state of natural Izu-Oshima basalts estimated by Mg-Fe partitioning between groundmass and plagioclase (Sato, 1989a, b).

The experimental run conditions are shown in Table 3. Table 4 presents the measurements of population density of plagioclase yielded by experimental run products. Table 4 indicates that the result of measurements are influenced somewhat by the method of analysis, especially for those of fine-grained samples. For example, for samples with a population density of plagioclase higher than 10^8 cm^{-3}, back-scattered electron images (BSI) give larger number densities than those obtained using optical microscope (OPT). This observation probably relates to the fact that the section image of plagioclase microlites, based on purely two-dimensional BSI, apprears to be finer grained than that based on OPT in which we get a larger outline image of plagioclase microlites within a thickness of thin sections (20–30 μm thick). The apparent size inversely affects the calculation of three-dimensional population density from data of two-dimensional population density. Therefore, the use of BSI is preferred in determination of the population density of plagioclase for fine-grained samples.

The results of the run products of the linear-cooling experiments are shown in Figs. 6 and 7. The charge is first melted and held at 1200°C for 1 or 10 hours, then cooled at constant rate down to 1100 or 1050°C, at which the charge is quenched in air or in water. Variation of the cooling rate from 10 to 1800°C/h caused only less than one order of magnitude difference in the population density of plagioclase (Fig. 7). For starting sample A, the population density varied from $10^{9.0}$ to

Table 4
Measurement of number density of plagioclase (Z) in the experimental run products

Run number	No.	Area (mm^2)	l_1 (μm)	l_2 (μm)	α	r (μm)	vol.%[a]	log(Z) (cm^{-3})	Method[b]
Linear cooling experiments									
#183A	2	2.35	49.3	123.4	5.36	38.1	0.41	4.5	OPT
#182A	14	2.36	27.7	67.3	2.29	23.5	1.31	5.2	OPT
#176A	7	2.36	15.5	24.5	1.66	10.9	0.12	5.1	OPT
#177A	164	0.0272	2.8	5.9	2.52	2.17	15.7	9.4	BSI
#184A	300	0.0087	1.0	2.4	2.43	0.84	18.3	10.5	BSI
#183B	91	0.0374	5.1	10.2	2.34	3.88	20.8	9.0	BSI
#183B	61	0.0421	7.0	17.0	2.59	6.02	20.6	8.2	OPT
#176B	67	0.0125	4.7	10.1	2.40	3.74	39.4	9.3	BSI
#176B	60	0.0189	6.5	16.6	3.08	5.60	36.1	8.7	OPT
#175B	89	0.0243	3.4	8.9	2.80	2.94	17.1	9.3	BSI
#175B	84	0.0363	7.4	17.6	2.73	6.27	32.7	8.4	OPT
#178B	133	0.1085	7.4	16.0	2.67	5.87	17.3	8.2	BSI
#178B	109	0.1763	9.1	36.0	4.48	9.70	20.6	7.9	OPT
#179B	153	0.0102	2.4	4.9	2.30	1.88	23.8	9.7	BSI
#179B	71	0.0188	6.2	19.0	3.43	5.91	44.9	8.8	OPT
Isothermal experiments									
#187A	13	2.35	35.0	88.2	2.29	30.3	2.0	5.2	OPT
#186A	51	1.017	31.3	111.2	3.80	31.9	20.1	6.2	BSI
#186A	57	2.33	42.4	168.8	4.35	44.5	19.5	6.5	OPT
#188A	70	0.0549	8.3	16.0	2.20	6.32	20.2	8.1	BSI
#180A	201	0.175	7.3	23.1	3.50	6.90	23.3	8.3	BSI
#180A	76	0.175	8.9	29.8	3.94	5.72	12.3	7.7	OPT
#185A	206	0.0095	1.3	4.2	3.53	1.21	19.3	10.5	BSI
#189A	179	0.0101	1.7	4.5	2.74	1.47	21.4	9.9	BSI

[a] Include void within plagioclase crystal.
[b] OPT = optical microscope; BSI = back-scattered electron image; No. = number of crystals measured; l_1 = mean width; l_2 = mean length; α = mean aspect ratio; r = average geometric-mean radius.

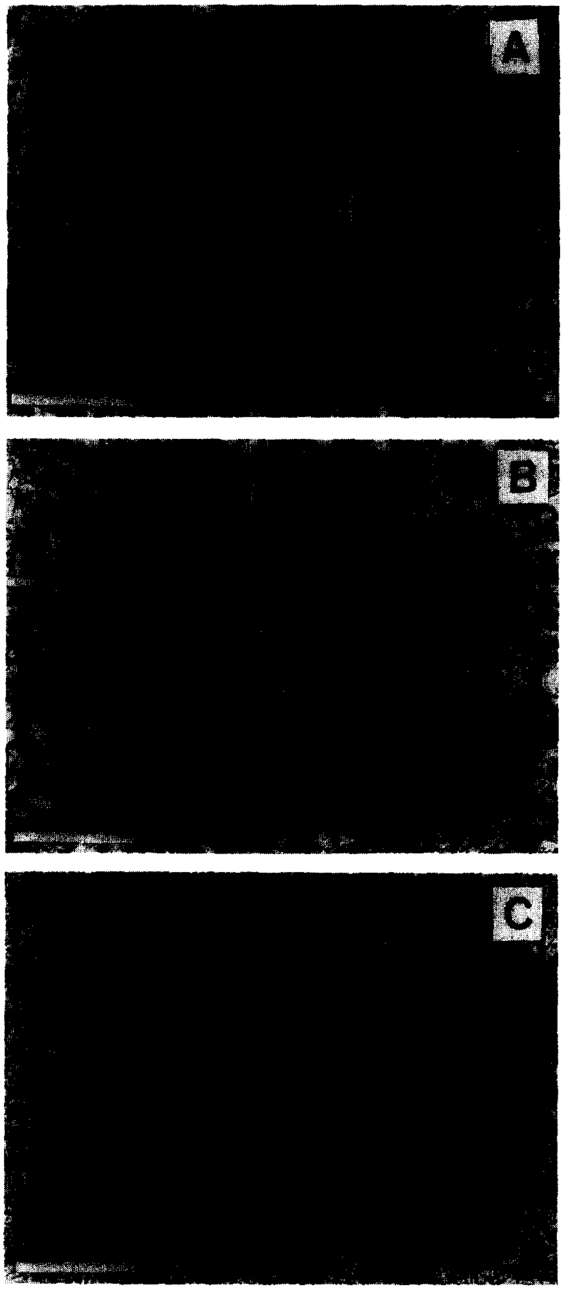

Fig. 6. Photomicrographs of the charges used in linear cooling experiments. Bars (lower left corner) are 0.1 mm; starting material A (Table 2). (A) Run number #183B in Tables 3 and 4. (B) #176B. (C) #179B.

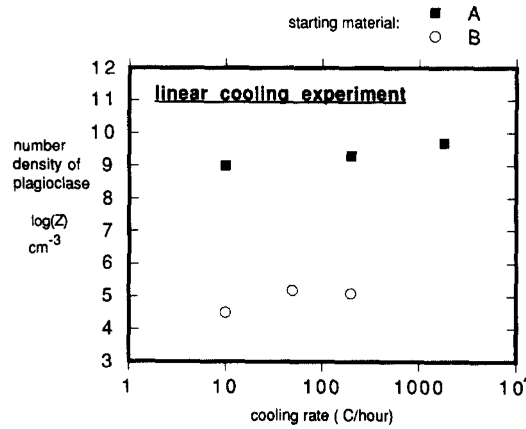

Fig. 7. Effect of cooling rate on the number density of plagioclase. ■ represent data on starting material *A* and ○ denote data on starting material *B*. More than two orders of magnitude difference in cooling rate apparently does not cause even one order of magnitude difference in the number density. Large differences in the number density of plagioclase for samples *A* and *B* result from differences in liquidus temperatures of the samples; for *A*, the liquidus temperature is ca. 1210°C and for *B* 1190°C.

$10^{9.7}$ cm^{-3}, whereas for starting sample B, it ranged from $10^{4.5}$ to $10^{5.2}$ cm^{-3}. The large departure of the population density of plagioclase in runs using samples A and B may be the result of a slight difference in the initial undercooling or superheating relative to their liquidus temperatures. The liquidus temperatures of the starting samples A and B are approximately 1210 and 1190°C, respectively. In Fig. 6 is shown that rapidly cooled charges contained thinner plagioclase laths than those cooled more slowly. Moreover, the difference in duration of initial melting — 1 versus 10 hours — did not cause much difference in the population density obtained (#176B and #175B, respectively, in Table 4), indicating that the 1-hour duration is sufficient to dissociate and equilibrate the melt structure.

Photomicrographs and back-scattered electron images of the run products of the isothermal-cooling experiment are shown in Figs. 8 and 9. These experiments are intended to examine the effect of initial-melting temperatures relative to the liquidus temperatures on the population density of plagioclase after annealing at 1100°C (Fig. 10). Starting material B (Table 2) is used for the isothermal crystallization experiments. The charge is first melted at variable T_0 for 1 hour, then cooled down to 1100°C within ca. 5 minutes. Care was taken not to undershoot nor overshoot during the thermal treatments. The charges were then kept at 1100°C for 1 or ca. 13 hours for crystallization, and then quenched. For runs with an initial-

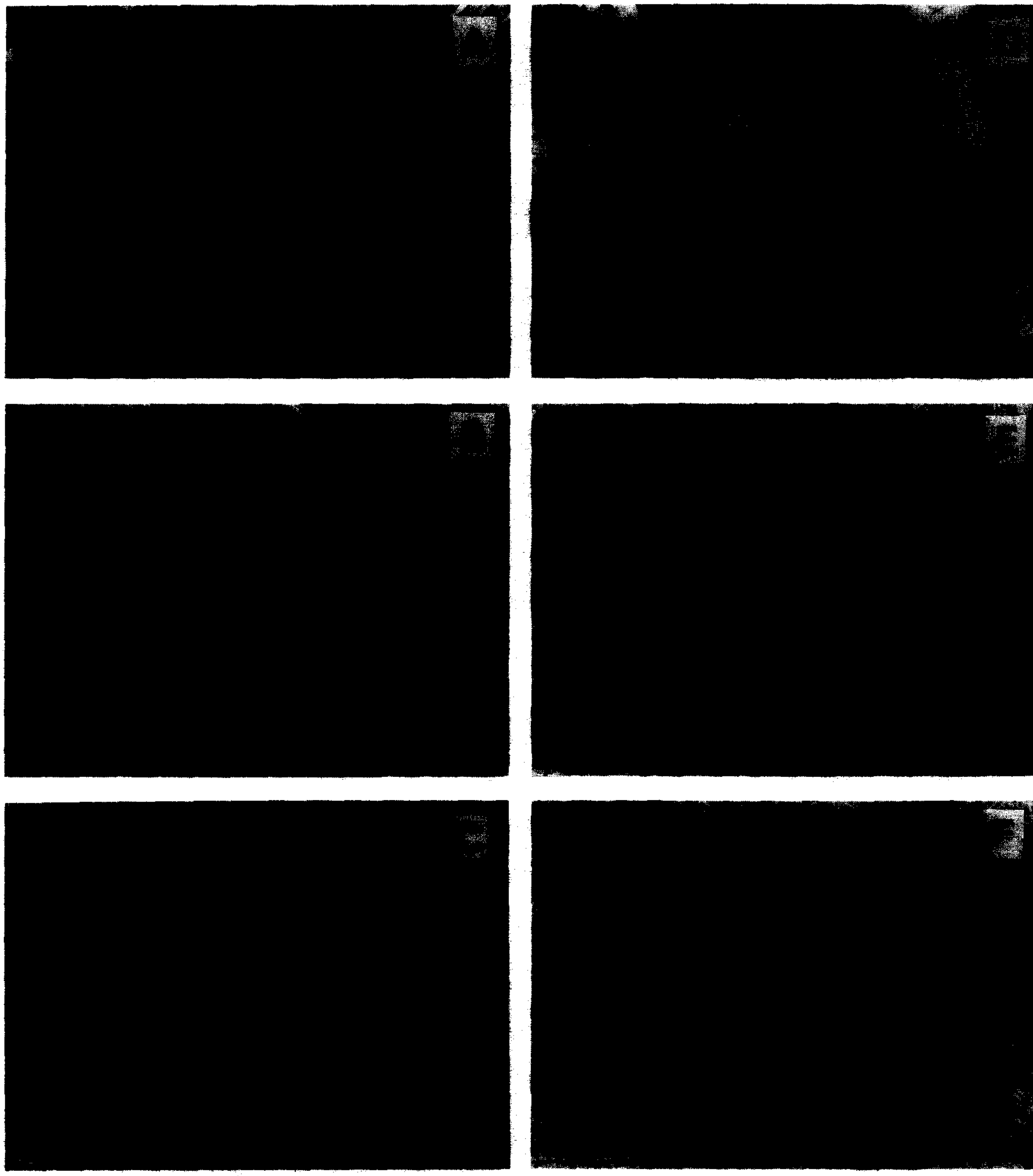

Fig. 8. Photomicrographs of the charges of isothermal crystallization experiments with variable initial-melting temperatures near the liquidus temperature for starting material B (liquidus temperature is 1190°C). Bars are 0.1 mm. (A–C) represent runs with 1-hour crystallization period at 1100°C and (D–F) show run products of ca. 13 hours of crystallization period at 1100°C. (A) #187A, T_0 = 1200°C. (B) #188A, T_0 = 1190°C. (C) #185A, T_0 = 1180°C. (D) #186A, T_0 = 1200°C. (E) #180A, T_0 = 1190°C. (F) #189A, T_0 = 1180°C.

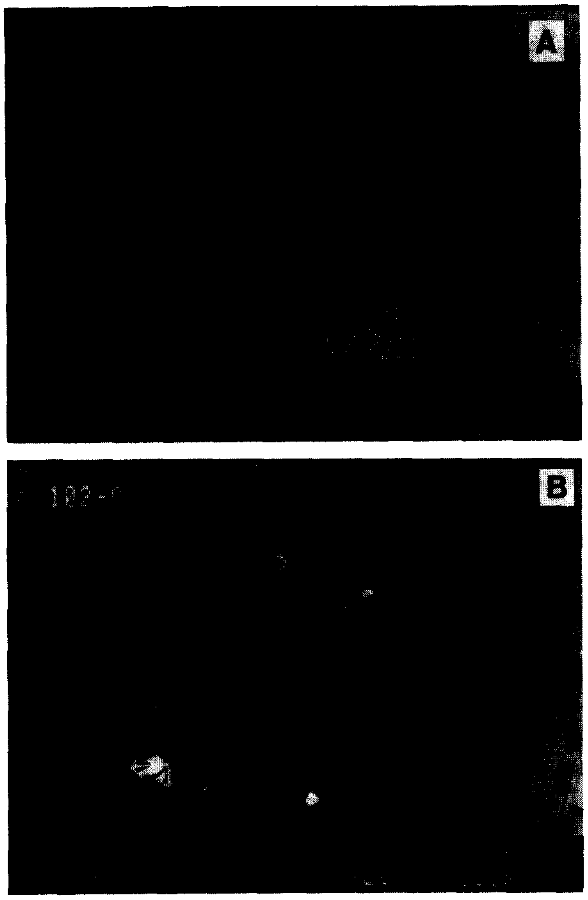

Fig. 9. Back-scattered electron images (BSI) of the run products of isothermal-crystallization experiments. Starting material B is used. (A) #188A, plagioclase + glass (annealing period—1 hour). (B) #180A, plagioclase + pigeonite + magnetite + glass (annealing period—13 hours).

melting temperature of 1200°C, ca. 10°C above the liquidus temperature, the run products are coarse grained and have a population density of $10^{5.2}$ and $10^{6.2}$ cm^{-3}. Run products with the annealing period of 1 hour at 1100°C contained only plagioclase and glass (Fig. 8A), whereas those with ca. 13 hours annealing time crystallized pigeonitic pyroxene and magnetite along with plagioclase (Fig. 8D). However, the population density of plagioclase is not affected by the duration period of annealing at 1100°C (Fig. 10), suggesting little nucleation within the charge after a 1-hour period of annealing at 1100°C. The plagioclase is commonly hollowed or fork-shaped skeletal (Figs. 8 and 9).

The population density of plagioclase is $10^{8.1}$–$10^{8.3}$ cm^{-3} for runs with an initial-melting temperature of 1190°C and $10^{9.9}$–$10^{10.5}$ cm^{-3} for runs with an initial-melting temperature of 1180°C. In Fig. 10 is demonstrated that only 20°C difference in the initial-melting temperature near the liquidus temperature causes more than five orders of magnitude difference in the population density of plagioclase. In run #189A, pyroxenes show chained crystal aggregates (Fig. 8F), suggesting that convection was minimum in the beads during the run. The apparent population density is uniform within each run product, and a homogeneous nucleation process dominated in all experiments. A charge melted at 1180°C and quenched directly from that temperature contained much less than 1% plagioclase crystal and showed a low population density of plagioclase, suggesting minimal effect of the relict plagioclase on the obtained population density.

Collectively, the experiments verified quantitatively that plagioclase nucleation is affected largely by the initial-melting temperature relative to the liquidus temperature, and is less dependent on the cooling rate for basaltic rocks of Izu-Oshima volcano. Below, I discuss the atomic scale significance of the strong effect of the initial-melting temperature on the population density of plagioclase demonstrated by the experiments, and an interpretation for the origin of the difference

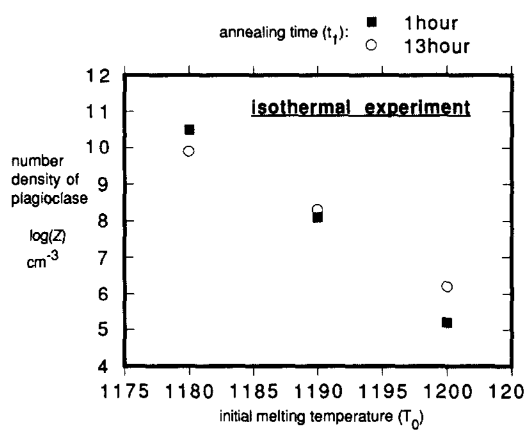

Fig. 10. Effect of initial-melting temperature near the liquidus temperature on the number density of plagioclase for starting material B. Note that number density of plagioclase does not seem to increase after one hour of crystallization at 1100°C. Only data obtained by BSI image were used except for data at 1200°C.

between groundmass textures of the pahoehoe and aa lavas of Izu-Oshima volcano.

5. Discussion

5.1. Effect of the initial-melting temperature on the population density of plagioclase

Delay of nucleation of plagioclase from basaltic melts has been examined experimentally by Gibb (1974), Lofgren (1980, 1983) and Tsuchiyama (1983). They showed that the initial degree of superheating of the melt is the dominant factor controlling plagioclase nucleation. Tsuchiyma attributes this effect to the large relaxation time of silicate melts in the nucleation of plagioclase. Kirkpatrick (1983) also pointed out the difficulty of the change of silicate melt structure for plagioclase nucleation. Nucleation of plagioclase requires polymerization of silicate melt, which is accompanied by large activation energy. The strong effect of the initial-melting temperature near the liquidus temperature on the population density of plagioclase in my experiments is interpreted as follows.

The number of crystal nuclei generated can be represented by the number of clusters in the melt larger than a critical size. The critical size of nuclei (R_c) is expressed by the equation $R_c = -2s/\Delta G_v$, where s and ΔG_v denote surface free energy and chemical free energy change per unit volume transformed (e.g., Kirkpatrick, 1981). Because chemical free energy difference between solid and liquid is roughly proportional to the degree of undercooling, critical size of nuclei is inversely correlated with degree of undercooling. On the other hand, equilibrium distribution (number per unit volume) of clusters in a melt is given by the Boltzmann distribution, i.e., $N_i = N_v \exp(-\Delta G/RT)$, where N_i is the number of clusters per unit volume containing i atoms, N_v is the number of atoms per unit volume of reactant phase, ΔG_i is the free energy of a cluster containing i atoms, R is the gas constant and T is the absolute temperature. Near the liquidus temperature slight increase of temperature brings about the smaller size distribution of the clusters. It is also pointed out that, near the liquidus temperature, nucleation rarely takes place because of the large critical size of nuclei. In undercooling the charge to 1100°C, it is possible that cluster-size distribution of the melt nearly retains that of the initial-melting near the liquidus temperature because of the long relaxation time of the structural change of melt. Under this condition, the critical size of nuclei becomes much smaller than the initial condition, and clusters with sizes larger than the critical size become nuclei to grow into visible crystals. Therefore, the population density in Fig. 10 approximately corresponds to the number of clusters in the initial melting of the charge larger than the critical size of nuclei at 1100°C. If the relaxation time of melt structure is short, cluster size distribution changes to the equilibrium one at 1100°C as the charge is cooled to that temperature, and the obtained population density should be independent of the initial-melting temperature. However, this is not in accord with the experimental results. Large effects of the initial-melting temperature on the nucleation of plagioclase have been demonstrated by other experiments (e.g., Gibb, 1974), and are also related to the long relaxation time of structural change (polymerization) of silicate melts. Preliminary experiments show that basaltic melt similar to that of Izu-Oshima, has a relaxation time of more than 300 hours in crystal nucleation near liquidus temperature (Hara and Sato, 1990).

Toramaru (1991) performed numerical simulation of crystallization in linearly cooling binary melts and showed that nucleation density is proportional to the 1.5 power of cooling rates. He assumed a homogeneous nucleation equation for diffusion-limited nucleation. The results of Toramaru's simulations are not in accord with the present experiments, which showed only a factor of 3 variation against 2.3 magnitude difference in cooling rate. This is probably due to the lack of consideration of large effects of relaxation of melt in plagioclase nucleation in Toramaru's simulation.

5.2. Difference in groundmass textures between the pahoehoe and aa lavas

The experimental results indicate that the observed two orders of magnitude difference in the population density of plagioclase between the pahoehoe and aa lavas of Izu-Oshima volcano cannot be caused simply by the difference in cooling rate. Instead, slight difference in the initial degree of undercooling of magmas can bring about large difference in the population density of plagioclase. In other words, the 1778 A.D. pahoehoe lava was fed from little undercooled magma pockets, whereas 1986 LA aa lava was under more undercooled conditions before final degassing and eruption. The undercooling of pre-eruptive magmas could be caused either by conductive heat loss or by degassing of magmas in the chamber. One possible model for degassing of pre-eruptive magmas is that associated with CO_2 degassing from the magma chamber. Gerlach and Graeber (1985) showed that Hawaiian basalts are oversaturated with CO_2 in the chamber (about 2 km depth), and degassing of CO_2 is accompanied by a little amount of H_2O degassing. Such degassing process may be operative in Izu-Oshima volcano, although we do not have data on the CO_2 contents of the basaltic magma. Another model for subsurface degassing is the convective degassing of magmas in the chamber and the conduit. Kazahaya et al. (1989) suggested that magma in the conduit is directly connected with the chamber, and degassing of volatiles may take place at the head of the magma conduit. The degassed magma becomes heavier and would be convectively overturned by the undegassed magmas from chambers. If this degassing model is taking place, the magmas in the chamber may be undercooled due to degassing, and would show high population density after eruption.

Another possible factor that influences the crystal nucleation in silicate melt is the effect of shear. Kouchi et al. (1986), using an infra-red heating furnace, demonstrated that stirring of melt increases the number of crystals in the basaltic charge, and reduces the incubation time of nucleation. Although their experiments included uncertainty as to the uniformity of temperature within the charge, it is possible that relaxation time of nucleation also would be reduced by the effect of shear, which generally increases the population density of plagioclase under larger undercooling. The observation of Rowland and Walker (1990) on the Hawaiian pahoehoe and aa lavas that aa lavas are accompanied by a high volumetric flow rate, whereas pahoehoe lavas occur when the volumetric flow rate is low, also suggests the possible effect of shear stress in the formation of aa and pahoehoe lavas. However, in the case of pahoehoe and aa lavas of Izu-Oshima volcano, there are no definite indications that effusion rate and advance rate of lava flow is related to the lava flow morphology. The 1778 pahoehoe lava flow of Izu-Oshima extends to northeastern part of the volcano for more than 6 km, and samples from both near the vent and the end of the lava flow have a similar small population density of plagioclase. The 1986LA aa lava is initially stored in the lava lake at the summit crater and flowed over for a small distance (less than 1 km) with low flow rate. Other lava flows of Izu-Oshima volcano do not show correlation between lava flow morphology and the scale of lava flow. These observations on the Izu-Oshima lavas suggest that large difference in the population density of plagioclase between the pahoehoe and the aa lavas is not entirely due to the effect of shear. Instead, available data suggest that the large difference in population density of plagioclase between pahoehoe and aa lavas of the Izu-Oshima volcano is determined mainly by the initial degree of undercooling before final degassing and eruption of magmas.

The linear slopes of the crystal size distributions in Fig. 3 may indicate rather constant nucleation and growth conditions of these lavas as discussed by Cashman (1990) and others. The difference in CSD slopes between the pahoehoe and aa lavas may represent much different nucleation and growth rates. However, the lavas have very similar bulk chemistry, thus precluding that nucleation and growth rates were significantly different. Furthermore, the present experimental work shows that nucleation is induced by reduction of the critical size of clusters in the melt. In natural systems the nucleation rate is controlled by the degassing rate through the increase of undercooling, which may not occur at constant rate. At present, I believe that the large difference in the CSD slopes for the pahoehoe and aa lavas (Fig. 3) reflects the difference in the nucleation density, and not a difference in growth rate.

Most of the run products in the isothermal-crystallization experiments contained skeletal hopper or fork-shaped plagioclase, although the outer surface retained a flat surface. This observation suggests that plagioclase initially grew under a diffusion-controlled process at ca. 100°C undercooling, and then surface-controlled growth predominated under less undercooled conditions because of the lowering of the liquidus temperature due to crystallization. In the natural lavas, plagioclases are often fork-shaped and show a flat surface, suggesting similar change of the conditions of crystallization, i.e., from diffusion-controlled rapid growth under high undercooling to surface-reaction-controlled slow growth under relatively small undercooling. Rapid degassing of basaltic magmas upon eruption may induce large undercooling of magmas, and cause rapid nucleation and growth of skeletal plagioclase microlites.

6. Conclusions

(1) Population densities of plagioclase in pahoehoe and aa lavas of Izu-Oshima volcano are $10^{7.0}$ and $10^{9.3}$ cm^{-3}, respectively. The mean size of plagioclase is about four times larger in the pahoehoe lavas than in the aa lavas, even though these lavas have similar groundmass chemical compositions.

(2) One-atmosphere melting/crystallization experiments simulating the time-undercooling relation of eruption show that cooling rate in a range of 10^{1}–$10^{3.3}$°C/h causes only threefold difference in population density of plagioclase, whereas 20°C difference in the initial-melting temperature near liquidus temperature causes about five orders of magnitude difference in the population density. This results mainly from the very large relaxation time of basaltic melt in the formation of crystal nuclei.

(3) It is most likely that, compared to the aa lavas, the pahoehoe lavas were formed from magmas with smaller initial undercooling before final degassing and eruptions.

Acknowledgements

The author is grateful for helpful comments on the manuscript by Dr. R. Tilling, Dr. Ritsuo Morishita and an anonymous reviewer, and discussions with Dr. A. Toramaru. Mr. Asao Minami is acknowledged for the help in BSI work. This study is partly supported by Scientific Grants of the Ministry of Education, Science and Culture of Japan.

References

Aramaki, S., 1971. Hydrothermal determination of temperature and water pressure of the magma of Aira caldera, Japan. Am. Mineral., 56: 1760–1768.

Aramaki, S., 1975. Classification and mechanism of volcanic eruptions. Bull. Volcanol. Soc. Jpn., 20: 205–221 (in Japanese with English abstract).

Blake, S., 1984. Volatile oversaturation during the evolution of silicic chambers as an eruption trigger. J. Geophys. Res., 89: 8237–8244.

Burnham, C.W., 1974. $NaAlSi_3O_8$–H_2O solutions; A thermodynamic model for hydrous magmas. Bull. Soc. Fr. Mineral. Cristallogr., 97: 223–230.

Cashman, K.V., 1988. Crystallization of Mount St. Helens 1980–1986 dacite: A quantitative textural approach. Bull. Volcanol., 50: 194–209.

Cashman, K.V., 1990. Textural constraints on the kinetics of crystallization of igneous rocks. Rev. Mineral., 24: 259–314.

Cashman, K.V. and Marsh, B.D., 1988. Crystal size distribution (CSD) in rocks and the kinetics and dynamics of crystallization II: Makaopuhi lava lake. Contrib. Mineral. Petrol., 99: 292–305.

Degraff, J.M., Long, P.E. and Aydin, A., 1989. Use of joint-growth directions and rock textures to infer thermal regimes during solidification of basaltic lava flows. J. Volcanol. Geotherm. Res., 38: 309–324.

Gerlach, T.M. and Graeber, E.J., 1985. Volatile budget of Kilauea volcano. Nature, 313: 273–277.

Gibb, F.G.F., 1974. Supercooling and crystallization of plagioclase from a basaltic magma. Mineral. Mag., 39: 641–653.

Gray, N.H., 1970. Crystal growth and nucleation in two large diabase dikes. Can. J. Earth Sci., 7: 366–375.

Gray, N.H., 1978. Nucleation and growth of plagioclase, Makaopuhi and Alae lava lakes, Kilauea volcano, Hawaii: discussion. Bull. Geol. Soc. Am., 89: 797–798.

Hara, I. and Sato, H., 1990. 1-atmosphere melting experiments on basalts of 1707 eruption product of Fuji volcano. Abstr. Volcanol. Soc. Jpn., 1990(2): 22 (in Japanese).

Ida, Y., 1990. Conditions to start volcanic eruptions. Bull. Volcanol. Soc. Jpn., 35: 299–312 (in Japanese with English abstract).

Jaupart, C. and Allegre, C.J., 1991. Gas content, eruption rate and instabilities of eruption regime in silicic volcanoes. Earth Planet. Sci. Lett., 102: 413–429.

Kazahaya, K., Takahashi, M., Shinohara, H. and Hirabayashi, J., 1989. Convective degassing of magmas at Izu-Oshima volcano. Abstr. Volcanol. Soc. Jpn., 1989(1): 24 (in Japanese).

Kilburn, C.R.J., 1981. Pahoehoe and Aa lavas: A discussion and continuation of the model of Peterson and Tilling. J. Volcanol. Geotherm. Res., 11: 373–382.

Kilburn, C.R.J., 1987. Rheological implications of the pahoehoe–aa transition in lavas. Abstr. Int. Union of Geodesy and Geophysics, 19th General Assembly, Vancouver, 2: 418.

Kirkpatrick, R.J., 1978. Nucleation and growth of plagioclase, Makaopuhi and Alae lava lakes, Kilauea volcano, Hawaii: reply. Bull. Geol. Soc. Am., 89: 799–800.

Kirkpatrick, R.J., 1981. Kinetics and crystallization of igneous rocks. Rev. Mineral., 8: 321–398.

Kirkpatrick, R.J., 1983. Theory of nucleation in silicate melts. Am. Mineral., 68, 66–77.

Kouchi, A., Tsuchiyama, A. and Sunagawa, I., 1986. Effect of stirring on crystallization kinetics of basalt: texture and element partitioning. Contrib. Mineral. Petrol., 93: 426–438.

Lipman, P.W., Banks, N.G. and Rhodes, J.M., 1985. Degassing-induced crystallization of basalt magma and its effects on lava rheology. Nature, 317: 604–607.

Lofgren, G.E., 1980. Experimental studies on the dynamic crystallization of silicate melts. In: R.B. Hargraves (Editor), Physics of Magmatic Processes. Princeton Univ. Press, Princeton, NJ, pp. 487–551.

Lofgren, G.E., 1983. Effect of heterogeneous nucleation on basaltic textures: a dynamic crystallization study. J. Petrol., 24: 229–255.

Macdonald, G.A., 1972. Volcanoes. Prentice-Hall, Englewood Cliffs, NJ, 510 pp.

Mangan, M.T., 1990. Crystal size distribution systematics and the determination of magma storage times: The 1959 eruption of Kilauea volcano, Hawaii. J. Volcanol. Geotherm. Res., 44: 295–302.

Marsh, B.D., 1988. Crystal size distribution (CSD) in rocks and the kinetics and dynamics of crystallization I. Theory. Contrib. Mineral. Petrol., 99: 277–291.

Nakamura, K., 1964. Volcano-stratigraphic study of Oshima volcano, Izu. Bull. Earthquake Res. Inst., Univ. Tokyo, 42: 649–728.

Nakano, S. and Yamamoto, T., 1991. Chemical variations of magmas at Izu-Oshima volcano, Japan: plagioclase-controlled and differentiated magmas. Bull. Volcanol., 53: 112–120.

Nicholls, J. and Stout, M.Z., 1982. Heat effects of assimilation, crystallization and vesiculation in magmas. Contrib. Mineral. Petrol., 81: 328–339.

Peterson, D.W. and Tilling, R.I., 1980. Transition of basaltic lava from pahoehoe to aa, Kilauea volcano, Hawaii: field observations and key factors. J. Volcanol. Geotherm. Res., 7: 271–293.

Presnall, D.C. and Brenner, N.L., 1974. A method for studying iron silicate liquids under reducing conditions with negligible iron loss. Geochim. Cosmochim. Acta, 38: 1785–1788.

Rowland, S.K. and Walker, G.P.L., 1990. Pahoehoe and aa in Hawaii: volumetric flow rate controls the lava structure. Bull. Volcanol., 52: 615–628.

Rutherford, M.J., Sigurdsson, H., Carey, S. and Davis, A., 1985. The May 18, 1980, eruption of Mount St.Helens 1. Melt composition and experimental phase equilibria. J. Geophys. Res., 90: 2929–2947.

Sato, H., 1989a. Redox states of magmas estimated by Mg-Fe partitioning between plagioclase and magma. Abstr. 28th Int. Geol. Congr., Washington, DC, 3: 28–29.

Sato, H., 1989b. Mg-Fe partitioning between plagioclase and liquid in basalts of Hole 504B, ODP Leg 111: a study of melting at 1 atm. Proc. ODP Sci. Results, 111: 17–26.

Sekine, T., Katsura, T. and Aramaki, S., 1979. Water saturated phase relations of some andesites with application to the estimation of the initial temperature and water pressure at the time of eruption. Geochim. Cosmochim. Acta, 43: 1367–1376.

Sparks, R.S.J. and Pinkerton, H., 1978. Effect of degassing on rheology of basaltic lava. Nature, 276: 385–386.

Stolper, E. and Holloway, J.R., 1988. Experimental determination of the solubility of carbon dioxide in molten basalt at low pressure. Earth Planet. Sci. Lett., 87: 397–408.

Swanson, S.E., Tanney, M., Westrich, H.R. and Eichelberger, J.D., 1989. Crystallization history of Obsidian dome, Inyo Domes. Bull. Volcanol., 51: 161–176.

Toramaru, A., 1991. Model of nucleation and growth of crystals in cooling magmas. Contrib. Mineral. Petrol., 108: 106–117.

Tsuchiyama, A., 1983. Crystallization kinetics in the system $CaMgSi_2O_6$–$CaAl_2Si_2O_8$: the delay in nucleation of diopside and anorthite. Am. Mineral., 68: 687–698.